East European Journal of Physics. 3. 617-628 (2026)
DOI:10.26565/2312-4334-2026-3-57 ISSN 2312-4334

ELECTRICAL, MECHANICAL AND OPTICAL PROPERTIES OF POLYAMIDE-6 COMPOSITES WITH CARBON NANOTUBES UNDER IRRADIATION

T.M. Pinchuk-Rugal[1], O.P. Dmytrenko[1], M.P. Kulish[1], A.I. Misiura[1,2]*, A.I. Momot[1], M.A. Alieksandrov[3], I. M. Danylenko[3], Yu.A. Onanko[4], O.M. Melnychenko[5]

[1]*Taras Shevchenko National University of Kyiv, 64, Volodymyrska St., 01033 Kyiv, Ukraine*
[2]*E.O. Paton Electric Welding Institute of NAS of Ukraine, 11 Kazymyra Malevycha St., 03680 Kyiv, Ukraine*
[3]*V.E. Lashkaryov Institute of Semiconductor Physics of NAS of Ukraine, 41, Nauky ave., Kyiv, 03028, Ukraine*
[4]*Department of Drainage, Institute of Water Problems and Land Reclamation of the National Academy of Agrarian Sciences of Ukraine, 37 Vasylkivska Str., Kyiv, 03022, Ukraine*
[5]*SE "RADMA", L.V. Pisarzhevsky Institute of Physical Chemistry of NAS of Ukraine, 31, pr. Nauky Ave., 03680 Kyiv, Ukraine*
**Corresponding Author e-mail: andrii_misiura@ukr.net*
Received March 26, 2026; revised August 15, 2026; accepted August 28, 2026

The dependence of the degree of crystallinity, the dynamic mechanical modulus, and the shear at frequency of ~1 MHz on the content of nanotubes was investigated for unirradiated PA-6/MWCNT nanocomposites. An increase in the degree of crystallinity and a decrease in these moduli with increasing CNT content were found, which is explained by the fact that CNTs in the polymer matrix act as nucleation centers of the crystalline *α*-phase, as well as nanoparticles disrupting interatomic bonds in chains and between macromolecules. These nanocomposites were irradiated with electrons $E_e \approx 1.8$ MeV and an absorption dose of 10 MRad (100 kGy), 20 MRad (200 kGy). The dependence of electrical conductivity, dynamic mechanical moduli, Raman scattering, and fast photoluminescence emission on the CNT content was measured. Irradiation has been shown to have complex effects on the properties mentioned above. Electrons can contribute to both the destruction of chains and the establishment of the crystalline phase, as well as the healing of damage caused by nanotubes through the recombination of electrons with free radicals. Radiation functionalization often leads to changes in the Raman spectra and the energy structure of electrons within the band gap. These changes are associated with the presence of local states related to the amorphous phase and structural defects. The restructuring of the FL spectra can also be affected, potentially impacting the formation of the conducting cluster.
Keywords: *Polyamide-6; Nanocomposites; Electrical conductivity; Degree of crystallinity; Dynamic moduli; Raman spectra; Fluorescence; Electron irradiation*

1. INTRODUCTION

Polyamides belong to a widespread class of acyclic and alicyclic polymers that include alkanes and amide groups –*NH–C–O*. These polymers have a simpler molecular structure with single numbering [1] and a more complex structure defined by double numbering [2]. The presence of polypeptide bonds in polyamides resembles the structure of proteins, and therefore, such polymers can serve as a model for studying the structural features of these biosystems. Among polyamides, polyamide-6 (PA-6, nylon-6) is the most affordable and widely used in various industries, especially in textiles and medicine. Polyamide-6 is characterized by a wide range of important physical and mechanical properties and high thermal and chemical resistance.

PA-6 is susceptible to the formation and rearrangement of crystalline phases with temperature changes. Thus, upon rapid cooling from the melt to low temperatures, crystallization occurs, forming a metastable γ phase. Its peculiarity is the close values of the lattice basis parameters ($\overrightarrow{|a|} \approx \overrightarrow{|b|}$), due to the twisting of the macromolecular chains. When the temperature is increased to 130 °C, a transition to a more stable *α*-phase with a triclinic structure is observed. This phase is characterized by a significant difference in the lattice parameters $\overrightarrow{|a|} \neq \overrightarrow{|b|}$. At a Brill temperature of $T_{Brill} \approx 160$ °C, a Brill transition is observed in the α-phase, where $\overrightarrow{|a|} \approx \overrightarrow{|b|}$. In addition, a transition from the crystalline *α*-phase to the *α*-phase with a pseudohexagonal structure is possible with increasing temperature [3, 4]. In contrast to the *γ*-phase, for which X-ray diffraction shows the presence of only one peak at $2\theta = 21.5°$ for λ_{Cu}, a similar pattern indicates the appearance of two peaks 200 ($2\theta = 20.13°$) and 002/202 ($2\theta = 23.85°$) [5].

For PA-6 fibers, the crystallization temperature $T_c = 189$°C and the melting point corresponding to reheating $T_m = 222$°C, respectively, the melting enthalpy $\Delta H_{M2} = 52$ J/g [6]. The sintering temperature for the amorphous component is $T_g = 54$°C. The tensile modulus is 2590 MPa at an elongation of about 100%.

Physical properties of PA-6, whose molecular structure is given by:

$$[–NH–C–O–(CH_2)_5]_n$$

depend significantly on the presence of a polar group capable of forming an interchain hydrogen bond (N-H...O=C), which largely determines the crystal polymorphism. The presence of such bonds in the *α*-phase is accompanied by features of the sheet structure.

Cite as: T.M. Pinchuk-Rugal, O.P. Dmytrenko, M.P. Kulish, A.I. Misiura, A.I. Momot, M.A. Alieksandrov, I.M. Danylenko, Yu.A. Onanko, O.M. Melnychenko, East Eur. J. Phys. 3, 617 (2026), https://doi.org/10.26565/2312-4334-2026-3-57

The appearance of such sheets leads to the indicated asymmetry of the lattice base plane in comparison with its higher energy for the γ-phase. The presence of different phases of amide polar groups in the chains of hydrogen bonds between macromolecules indicates the possibility of a wide modification of PA-6 properties due to the structural and radiation functionalization of this polymer, which is accompanied by changes in the important properties of these materials. Numerous studies have shown that one of the potentially most important materials for structural functionalization of polyomides is multi-walled carbon nanotubes (MWCNTs), which are characterized by high strength, thermal and electrical conductivity, and are affordable nanostructures [7, 8]. A significant effect on the modification of polyamide properties also occurs when irradiated with γ-photons [9]. At the same time, most studies on the structural and radiative functionalization of polyamides are aimed at studying mechanical and calorimetric properties and, to some extent, various photophysical changes, such as fluorescence, which is of considerable interest.

The aim of this work is to study the electrical conductivity and optical properties of polyamide-6 and its composites with MWCNTs under radiation functionalization via high-energy electron irradiation, to establish the mechanisms underlying the modification of these properties with increasing dose rate.

2. MATERIALS AND METHODS

The composites investigated were based on polyamide 6 (PA-6) filled with multi-walled nanotubes (MWNTs). The composite samples were obtained by hot pressing; for this purpose, a mechanical mixture of polymer powder and nanotubes was placed in a closed metal mold at T = 230°C and an external pressure of 30 MPa. The samples were obtained as discs with a diameter of 30 mm and a thickness of approximately 2 mm. The concentrations were 0-0.015 vol. pt. of MWCNTs.

The crystal structure of PA-6/MWCNT nanocomposites was determined using an X-ray diffractometer (DRON-3 M) with monochromatic CuKα (λ = 0.154178 nm) radiation.

To investigate the mechanical properties of PA-MWCNT nanocomposites, a computerized ultrasonic velocity meter KERN-4 was used. The dynamic Young's modulus was determined by the formula $E = \rho V^2_l$, where ρ is the density of the sample, V_l is the velocity of quasi-longitudinal elastic ultrasonic waves. The dynamic shear modulus was obtained by the equation: $G = \rho V^2_{tr}$, where V_{tr} is the velocity of quasi-transverse ultrasonic elastic waves.

The Raman and FL spectra were recorded using a Horiba Jobin Yvon T64000 triple spectrometer (Japan) with Ar-Kr ion (λ_L=488 nm) and He-Cd (λ_L=325 nm) lasers, respectively. The measurements were performed at room temperature.

The electron irradiation was carried out with the linear accelerator ILU-6 with energy E_e=1.8 MeV, absorption doses of 10 MRad (100 kGy) and 20 MRad (200 kGy) at the temperature T = 333 K.

3. RESULTS AND DISCUSSION

3.1. Quantum chemical calculations

Quantum chemical studies were performed on polyamide dimer and trimer molecules. Calculations were carried out using the Gaussian 09 software package and the density functional theory (DFT) method, with the B3LYP hybrid functional and 6-31G(d) basis set. Fig. 1-2 show the optimised geometry of the polyamide dimer and trimer molecules (one of the conformers).

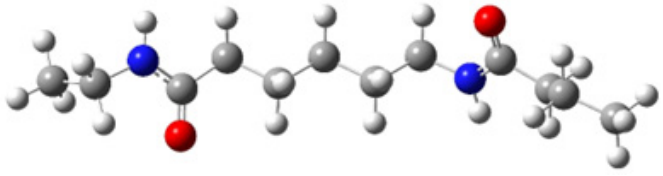

Figure 1. Optimized geometry of the polyamide dimer

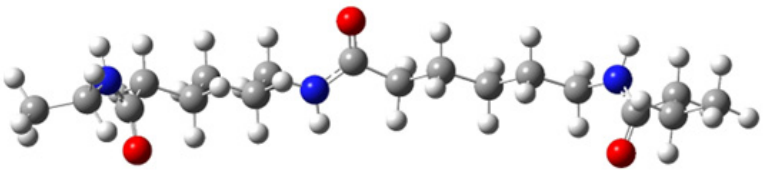

Figure 2. Optimized geometry of the polyamide trimmer

The natural vibrations of polyamide molecules were calculated. A scale factor of 0.9614 was applied to the frequencies [10]. As can be seen in Fig. 3, the Raman scattering spectra of the monomer, dimer, and trimer are almost identical. The valence vibrations of C=O and N–H are not sensitive to the length of the polymer chain and are found at frequencies of 1709 cm^{-1} and 3483±1 cm^{-1}. The broad band near 3000 cm^{-1} corresponds to the valence vibrations of C-H.

Figure 4 shows the calculated Raman scattering spectra resulting from the combination of polyamide molecules within the frequency range of 800–1,600 cm^{-1}.

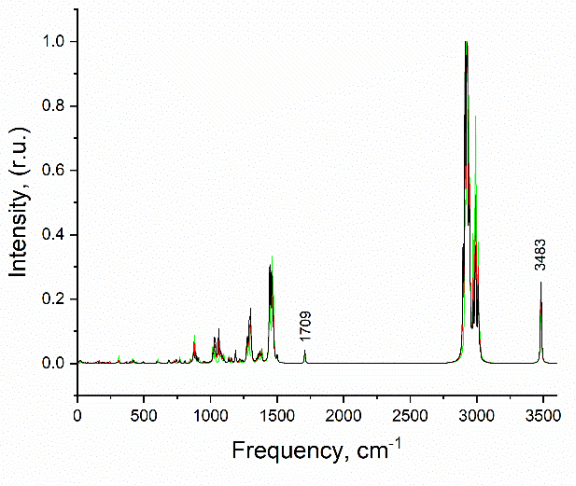

Figure 3. Raman scattering spectra for the monomer (green line), dimer (red line) and trimer (black line) of the polyamide

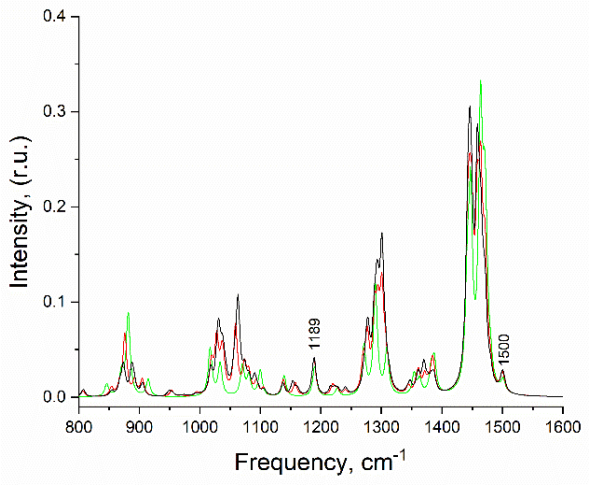

Figure 4. Raman scattering spectra of the monomer (green line), dimer (red line) and trimer (black line) of the polyamide, within the 800–1600 cm^{-1} range

Table 1 presents the calculated frequencies of the main fundamental oscillations of polyamide chains.

Table 1. Frequencies of the main fundamental oscillations of polyamide chains.

	monomer	dimer	trimer
	Frequency, cm^{-1}		
Valence vibrations N–H	3483	3482	3484
Valence vibrations C=O	1709	1709	1709
Deformation vibrations N–H	-	-	1500

3.2. Electrical conductivity and mechanical properties of PA-6-MWCNT nanocomposites

Filling PA-6 with nanotubes and increasing the concentration of nanotubes leads to a significant decrease in resistivity. While the resistivity of pure PA-6 is $\rho \approx 10^{13}$ Ω·cm, it drops to $1.4 \cdot 10^{7}$ Ω-cm at 6 wt.% CNT content and to $2.8 \cdot 10^{1}$ Ω·cm at 12 wt. % CNT content. A similar decrease in resistivity is also observed for other fillers, such as carbon black, but at higher concentrations [11].

The electrical conductivity at AC current (σ_{AC}) in the frequency range of 10^{-3}-10^{7} for pure PA-6 increases linearly, and with the addition of MWCNTs, regions of constant conductivity appear for $\sigma_{DC} = \sigma_{AC}$ at a nanotube concentration of 4 wt.%, the electrical conductivity is constant over the entire frequency range and is equal to $\sigma_{DC} = \sigma_{AC} = 10^{-3}$ S/cm. At the same time, the ratio of the intensities of the D- and G-bands inherent in MWCNTs changes. The behavior of σ_{AC} changes when not only MWCNTs but also N_a–A+A are added to PA-6. The latter compound improves the dispersion of the MWCNTs in the PA-6 matrix, as shown by TEM images. The improvement in dispersion is accompanied by an increase in σ_{DC} by several orders of magnitude [12]. The electrical resistivity of PA-6 and other polyamides depends not only on the CNT content, but also on the mixing temperature of the components and the rotational speed during the mixing of the CNTs in the polymer matrix, which affects the filler dispersion index and, in turn, leads to changes in calorimetric parameters such as melting point, crystallization temperature and their enthalpies [13]. The electrical conductivity of filler networks is affected not only by the melt state but also by the crystallization of the polymer matrix [14].

Since the dispersion of the nanotubes plays a significant role in the electrical conductivity behavior, there are a large number of nanotube modifications for their grafting to macrochains of polymers, including PA-6. One of these methods involves the application of a thin layer of polyethylene to the surface of the CNTs. Such catalyzed polymerization of nanotubes allows not only to take advantage of the significant aspect ratio inherent in CNTs, but also to significantly improve their dispersion due to reduced aggregation while maintaining a low percolation threshold in nanocomposites. At the same time, the properties of PA-6/MWCNT nanocomposites are enhanced, allowing for their wide use in antistatic devices, in the production of sensors for absorbing electromagnetic radiation in radar applications, and in the production of conductive rubber. Thus, the percolation threshold for uncoated PA-6/ MWCNT nanocomposites is 0.4 wt. %, and for PA-6/ MWCNT nanocomposites (with polyethylene coating of the CNT surface) it decreases to 0.1 wt.%. The value of $\sigma_0 = 6.0 \cdot 10^{-5}$ S/cm for PA-6/MWCNT was significantly lower than $\sigma_0 = 3.0 \cdot 10^{-3}$ S/cm for PA-6/ MWCNT (coated with PE). These differences are explained by the morphology of the composites, depending on the modification of the polymer matrix and fillers, in which the matrix area separating the conductive nanotubes changes. As a consequence, the conductivity of the nanotubes in the matrix is attenuated by electron transfer through potential barriers present in the region of the conductive cluster. In addition to reducing the percolation threshold in PA-6/MWCNT nanocomposites (with a PE layer on the surface), the electrical conductivity at 1 wt.% MWCNT increases by eight orders of magnitude, and for the PA-6/MWCNT nanocomposite by only five orders of magnitude compared to pure PA-6.

The properties of PA-6/MWCNT nanocomposites are influenced not only by the modification of nanotubes aimed at improving their dispersion but also by the method of nanocomposite production, which involves the creation of a segregated heterophase structure of nanocomposites. This structure involves the formation of nanotube layers on the surface of polymer matrix blocks. For PE and PVC nanocomposites, a significant decrease in the percolation threshold is observed when these segregated structures are formed [15-19]. For other systems, such as PEG, and PPG, similar low values of φ_c have not been observed [20]. For PA-6/ MWCNT nanocomposites it is interesting to use the method of creating segregated structures. If the percolation thresholds for PE/MWCNT and PVC/MWCNT are $\varphi_{cPE} = 0.00099$ vol.pt. and $\varphi_{cPVC} = 0.0001$ vol.pt., respectively, then $\varphi_{cPA\text{-}6} = 0.041$ vol.pt. ($t=1.65$, $\sigma_0 = 2.24$ S/cm.) The electrical conductivity of pure PA-6 exceeds its known value of ~10^{-13} S/cm and is ~10^{-10} S/cm. In the region below the percolation interval, a slow increase in electrical conductivity is observed due to the jump charge transfer mechanism. In the percolation region, the increase in electrical conductivity is about six orders of magnitude, which is typical for systems with percolation behavior of conductivity. At the same time, the observed differences indicate the importance of the thermal history during the preparation of the nanocomposites and the absence of the expected segregated structure.

It can be assumed that the result obtained is a consequence of the peculiarities of the morphology of PA-6 and PA-6/MWCNT, which is different from other polymers in the formation of nanocomposites with CNTs.

Figure 5 shows the behavior of Young's modulus and dynamic mechanical properties obtained for the elastic state at a frequency of 1 MHz.

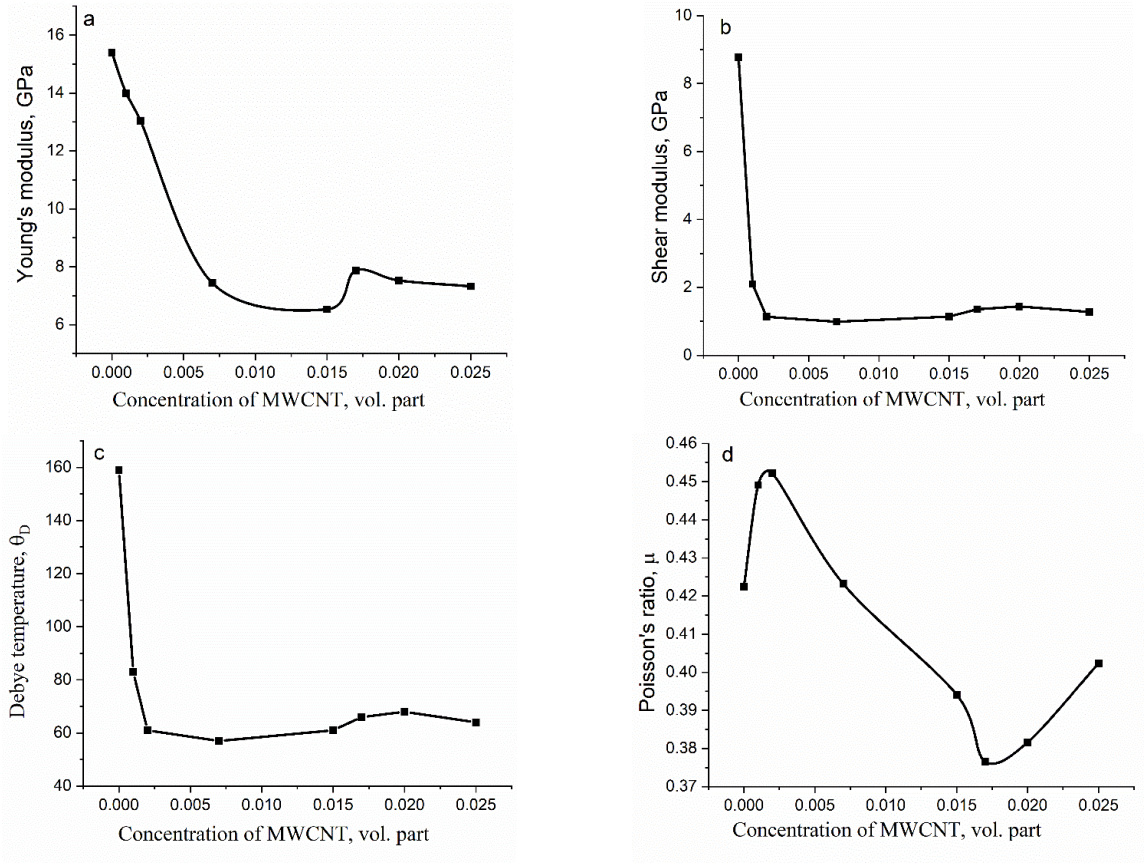

Figure 5. Dynamic moduli of Young's modulus (a) and shear (b), Poisson's ratio (c), Debye temperature (d) for PA-6/MWCNT composites at different filler locations in the elastic region at a sound frequency of 1 MHz

These dependencies differ from the behavior of the statistical modulus, which takes into account not only the elastic but also the relaxation properties of the deformation [11]. It can be seen that the highest values of the moduli occur for pure PA-6. With the addition of nanotubes, the elastic properties of polyamide deteriorate. A slight increase in the modulus occurs in the interval of conductive network formation. The presence of nanotubes may lead to the destruction of the structure of the previously established α-phase, which is also formed by hydrogen bonds. Another reason may be the interaction of nanotubes with amide groups of macrochains, which affects their elastic properties. On the other hand, the above-mentioned interaction with macromolecules and the crystalline phase can counteract the formation of agglomerates with nanotubes. This in turn helps the nanotubes to act as active centers of crystallite nucleation. As can be seen from Figure 6, the degree of crystallinity increases as the nanotube content increases.

If the degree of crystallinity increases slowly from 55 to 60 % at a low MWCNT content, then as the concentration of MWCNTs is further increased, the degree of crystallinity increases rapidly from 60 to 75 %. In the case of nanotube agglomeration, the opposite effect is expected. The significant values of the degree of crystallinity are noteworthy. The

presence of a large number of crystallites prevents the formation of a conductive cluster, which affects the increased values of the percolation threshold and a decrease in the increase of electrical conductivity in the percolation region. The absence of a segregated distribution of MWCNTs is also evidenced by the value of t = 1.65, which is close to the theoretical value of t = 2 in the random distribution of nanotubes. On the other hand, the unusual nature of electrical conductivity and mechanical properties is confirmed by the value of σ_0= 2.24 S/cm, although this value is significantly lower for most nanocomposites [21].

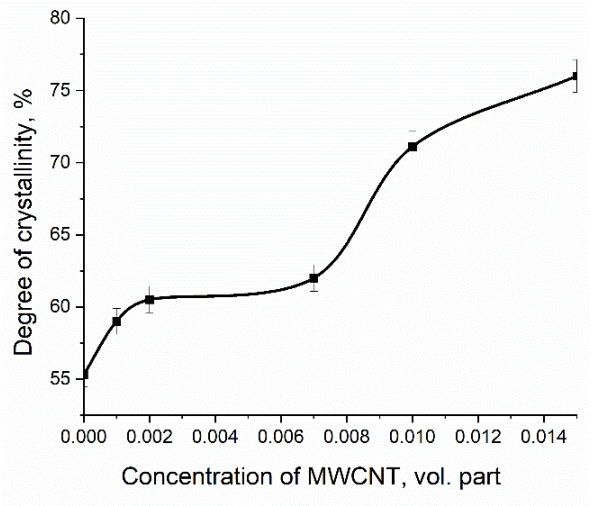

Figure 6. Dependence of the degree of crystallinity on the content of nanotubes in PA-6/ MWCNT composites

3.3. Radiation modification of the properties of PA-6 polyamide and PA-6/MWCNT nanocomposites

The peculiarities of the structure of polyamides, including PA-6, and the possibility of their modification within a wide range will allow them to be used to solve various problems. For example, by annealing at different temperatures, which allows to obtain different initial crystalline phases, it is possible to significantly influence the absorption in the THz range caused by vibrations parallel and perpendicular to the molecular chain [22]. The addition of certain additives can significantly increase the fire resistance [8]. Of interest is not only the filling of polyamides with CNTs, but also their deposition on the surface of polymers, since this makes it possible to create surfaces that do not trap proteins from the bloodstream, thus expanding the possibilities of using polyamides as implants in medicine [23]. A special place in modifying the properties of polyamides is occupied by radiation functionalization. Such functionalization is mainly performed using γ-irradiation or high-energy electron bombardment with different absorption doses.

Upon γ-irradiation of polyamide with 6,12 γ-photons with a dose increase from 0 to 300 kGy, an increase in the degree of crystallinity in the range of ~15 to ~19% is observed.

The melting point T_m undergoes a more complex restructuring at similar doses. At lower doses (up to ~50 kGy), T_m increases and after passing the maximum, it decreases. The study of the IR absorption spectra of samples irradiated with doses of 100 and 200 kGy, compared to the unirradiated ones, shows a significant restructuring of the spectra in the whole range, but mainly in the region of *N–H* valence vibrations in interchain hydrogen bonds and amide bands caused by vibrations in *–NH–C–O–* groups. These results indicate that an increase in the dose of γ-irradiation with an increase in the degree of crystallinity leads mainly to the destruction of crystallites [22]. In addition, γ-irradiation induces morphological changes in polyamides [23].

Comparison of Raman spectra for polyamide 6,12 irradiated with γ-photons at doses of 15, 50, 100, 200, and 300 kGy with unirradiated samples confirms the destruction of crystallites due to the destruction of molecular chains, which leads to an increase in the molar content of oligomers with increasing dose.

This chain degradation is mainly realized as a consequence of radiation damage to amide groups [2, 9]. Raman scattering for γ-irradiated crystalline samples in the form of PA 6,12 fibers depends on their orientation and temperature (dose of 50 kGy). At T ≈ 110°C, sharp changes in the intensities of the bands associated with the valence vibrations of the CH_2 and *C–C* groups are observed. Similar changes in intensity are observed for a temperature of 80 °C at different doses. The obtained results indicate that γ-irradiation affects not only the formation or degradation of crystallites but also changes the Brill transition point with the appearance of a stable modified γ-phase in the dose range from 50 to 100 kGy [24]. In the case of electron irradiation of PA-6 with an energy of 1.3 MeV and doses of 100, 200, 300, and 400 kGy at room temperature, there are noticeable changes in the intensity of many IR absorption bands.

The most significant changes are in the spectral regions caused by the vibrational modes of the amide, metal groups, *C–C* bonds, and *N–H* groups responsible for hydrogen bonding between the chains. It is important to note that the nature of these changes is not linearly related to the increase in dose. Exposure to different doses of PA-6 affects sample morphology, melting point T_m, melting enthalpy, and X-ray diffraction. If for an unirradiated sample T_m = 220 °C and melting enthalpy ΔH_M = 57.33 J/g, then these values decrease with increasing dose during irradiation, and at 400 kGy

they are equal to 215 °C and 27.52 J/g, respectively. The surface of spherulites is destroyed with increasing dose for irradiated samples. In addition, the diffraction peaks corresponding to the α-phase lose their intensity with increasing dose. These results indicate that electron irradiation reduces crystal properties [25].

3.3.1. Electrical conductivity and mechanical properties of radiation functionalized PA-6/MWCNT nanocomposites

Irradiation with electrons of energy E_e1.8 MeV leads to the formation of the simplest class of radiation defects, namely Frenkel pairs, and is accompanied by the appearance of free radicals due to the absence of dominant spontaneous recombination. It is shown that the appearance of radiation-stimulated radicals can lead to the rupture of bonds in the amide group of PA-6 chains, interchain hydrogen bonds, and cross-links in the region of methylene groups of CH_2. It is difficult to predict the mechanisms of radiation damage, but it is obvious that their priority depends on the dose level. At high doses, radiation degradation of materials can also be expected. In nanocomposites with MWCNTs, the situation is even more complicated due to the influence of incorporated nanotubes. At the same time, changes in the effect of nanotubes on the polymer matrix due to radiation defect formation in CNTs cannot be included [26, 27].

To interpret the results of radiation functionalization of PA-6/MWCNT nanocomposites in a wide dose interval of electron irradiation, it is advisable to extend the effect of low doses, e.g. 10-20 MRad (100-200 kGy).

Figure 7 shows the dependence of the electrical conductivity of the PA-6/MWCNT nanocomposite on the nanotube content after electron irradiation with a dose of 10 MRad and 20 MRad(100-200 kGy).

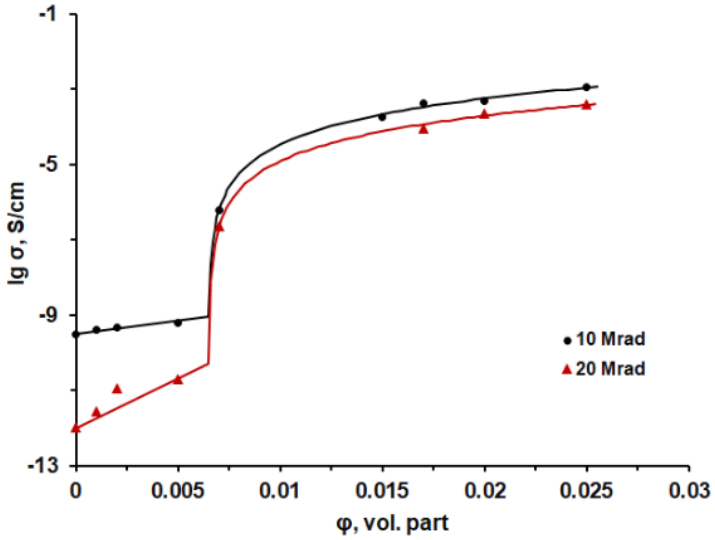

Figure 7. Dependence of the electrical conductivity at DC for PA-6/MWCNT nanocomposites on the content of nanotubes after electron irradiation (E=1.8 MeV) with an absorption dose of 10 MRad (100 kGy) and 20 MRad (200 kGy)

The use of the scaling dependence to describe the behavior of the electrical conductivity at constant current, σdc, yields result that differ from those obtained for PA-6/MWCNT nanocomposites without irradiation [28]. Thus, the following values were obtained for the composite irradiated with 10 MRad $\varphi_c = 0.0065$ vol. pt., $t = 2.08$, $\sigma_0 = 4.46$ S/cm. When this composite was irradiated with a dose of 20 MRad, the values obtained for the fitting parameters of the percolation equation were very close $\varphi_c = 0.0065$ vol. pt., $t = 2.06$, $\sigma_0 = 1.42$ S/cm.

The electrical conductivity in the percolation region increases by a jump of about four orders of magnitude. We observe a decrease in the percolation threshold and a slight decrease in electrical conductivity within the percolation region. Additionally, there is a more homogeneous filler distribution and a slight increase in σ_0. These changes result from structural transformations in the PA-6 polymer matrix under irradiation, which affect the formation of the conductive cluster. A decrease in the electrical conductivity of the composite after irradiation with a dose of 20 MRad in the pre-percolation region may indicate radiation-induced damage to polymer chains and the formation of defects that impair charge transfer.

Figure 8 shows the dynamic mechanical characteristics describing the elastic properties of PA-6/MWCNT nanocomposites irradiated with a dose of 10 MRad (100 kGy) and 20 MRad (200 kGy).

Although a slight decrease in the studied values is observed, the dependencies of mechanical characteristics on the absorbed dose of 20 Mrad remain similar. A radiation dose of 20 MRad is insufficient to cause significant changes to the mechanical properties of composites.

Compared with the results presented in Fig. 5, the changes in dynamic and shear moduli with increasing nanotube concentration are largely preserved relative to unirradiated composites and tend to decrease with increasing filler content. At the same time, the values of shear moduli for irradiated composites exceed those of unirradiated samples at higher nanotube contents.

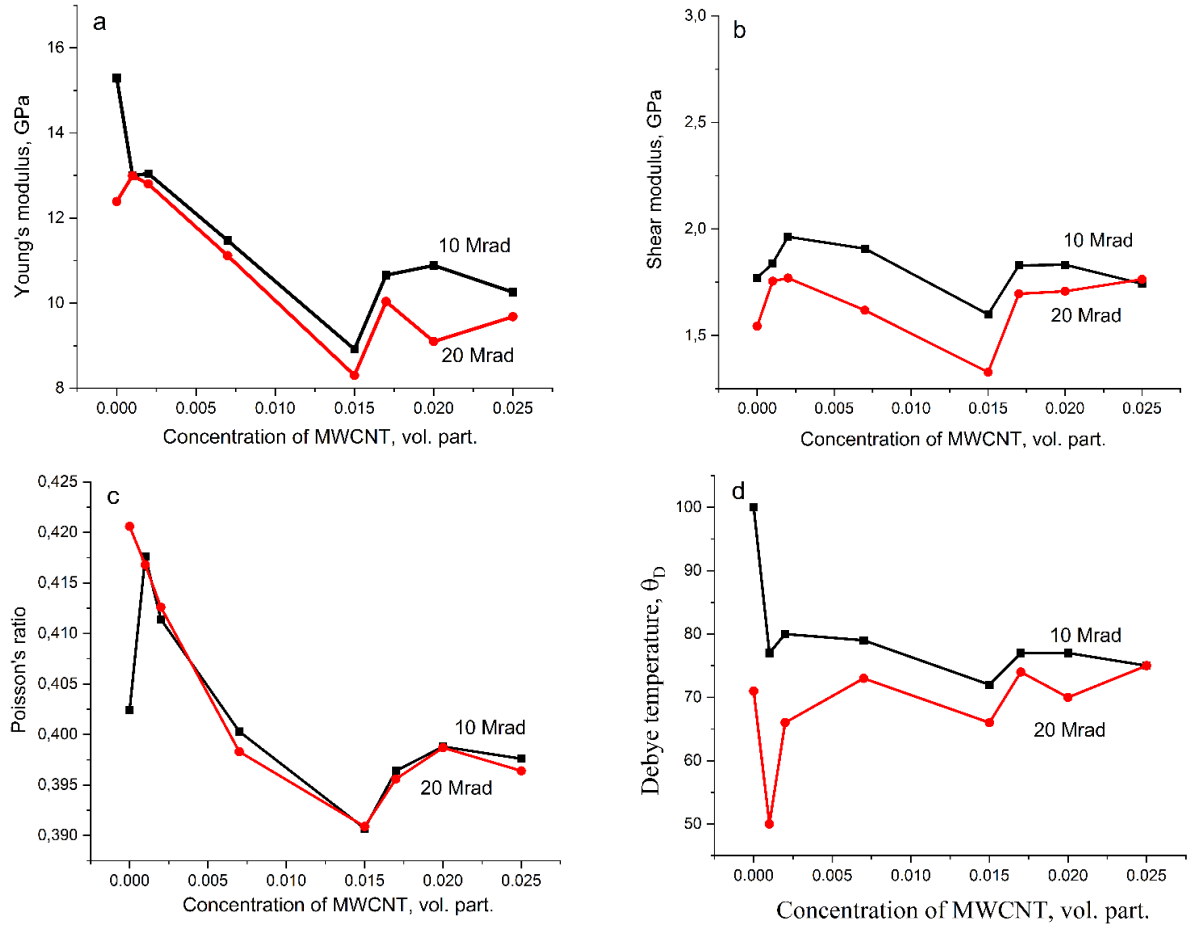

Figure 8. Dynamic Young's and shear moduli, Poisson's ratio, Debye temperature for PA-6/MWCNT composites at different filler locations after electron irradiation (E_e = 1.8 MeV) with an absorption dose of 10 MRad (100 kGy) and 20 MRad (200 kGy) in the elastic region at a sound frequency of 1 MHz

3.3.2. Raman scattering and fluorescence of radiation functionalized PA-6/MWCNT nanocomposites

For unirradiated PA-6/MWCNT nanocomposites, a significant Raman spectrum restructuring was observed with increasing nanotube content. Such changes occur for many bands of vibrational modes, especially those associated with valence vibrations of asymmetric and symmetric vibrations of CH_2 (2931, 2901, 2,871 cm^{-1}), amide-I ($C=O$), 1631 cm^{-1}), CH_2 (bending 1446 cm^{-1}), amide III (1276 cm^{-1}), valence stretching of $C–C$ (1121 cm^{-1}, etc.) [22].

Damage to the bonds within the chains by nanotubes contributes to a decrease in the elastic properties of the polymer matrix.

Irradiation of nanocomposites leads to an additional restructuring of the Raman spectra, which can be seen in Figure 9.

Compared to the unirradiated nanocomposite with 0.001 vol. pt. CNTs, irradiation resulted in slight changes in the scattering spectrum. At the same time, while maintaining the general picture of the bands, a slight shift of them is observed, for example, the amide I band from 1631 cm^{-1} to 1636 cm^{-1} and a redistribution of intensities, mainly for the valence vibrations of CH_2 groups. When a nanocomposite with 0.005 vol. pt. CNTs is irradiated, the spectrum returns to the appearance characteristic of nanocomposites with lower CNT content compared to the unirradiated one. While for the unirradiated sample, the most intense band is at 1306 cm^{-1} (CH_2 torsion), the less intense bands are at 1129 cm^{-1} ($C–C$ valence), 1443 cm^{-1} (CH_2 bending), 1639 cm^{-1} (amide I), for the irradiated nanocomposite the bands at 1125 cm^{-1}, 1445 cm^{-1}, 1636 cm^{-1} are more intense. Similar deviations in the shifts and relative intensities of the bands also occur for higher concentrations of MWCNTs.

Thus, the Raman spectra of each of the irradiated composites undergo changes indicating intramolecular vibrations of both nanotubes and radiation damage. At the same time, despite the general deterioration of the elastic properties induced by CNTs, a slight improvement is observed as a result of electron bombardment. The radiation damage may be insignificant at the chosen dose (100 kGy), and due to the recombination of electrons with free radicals formed as a result of the interaction of CNTs with the polymer matrix, the circuit damage is healed, leading to an improvement in the elastic properties of the matrix. Other mechanisms of influence of mechanical and radiation damage to the chains and their manifestations on the elastic properties of nanocomposites and the formation of conductive clusters in them are also possible. It is known that PA-6 polymers are characterized by fast fluorescence, i.e. delayed fluorescence (FL) with

backlighting. The fast fluorescence spectra for the α and γ crystalline phases are different and their appearance depends on the excitation wavelength. For example, when excited at λ_{ex} = 267 nm, the α phase band appears with emission maxima at 340 and 390 nm, and the maximum of the γ phase emission band is at 500 nm. Excitation at λ_{ex} = 400 nm gives the same spectra for both phases with a maximum of 480 nm. Changing λ_{ex} from 300 to 312 nm for the α-phase results in a switch in intensity from a band with a maximum of 340 nm to a band with a maximum of 390 nm. This behavior of fast FL is explained as a consequence of the recombination of photoinduced charges with an almost continuous energy distribution [24, 25].

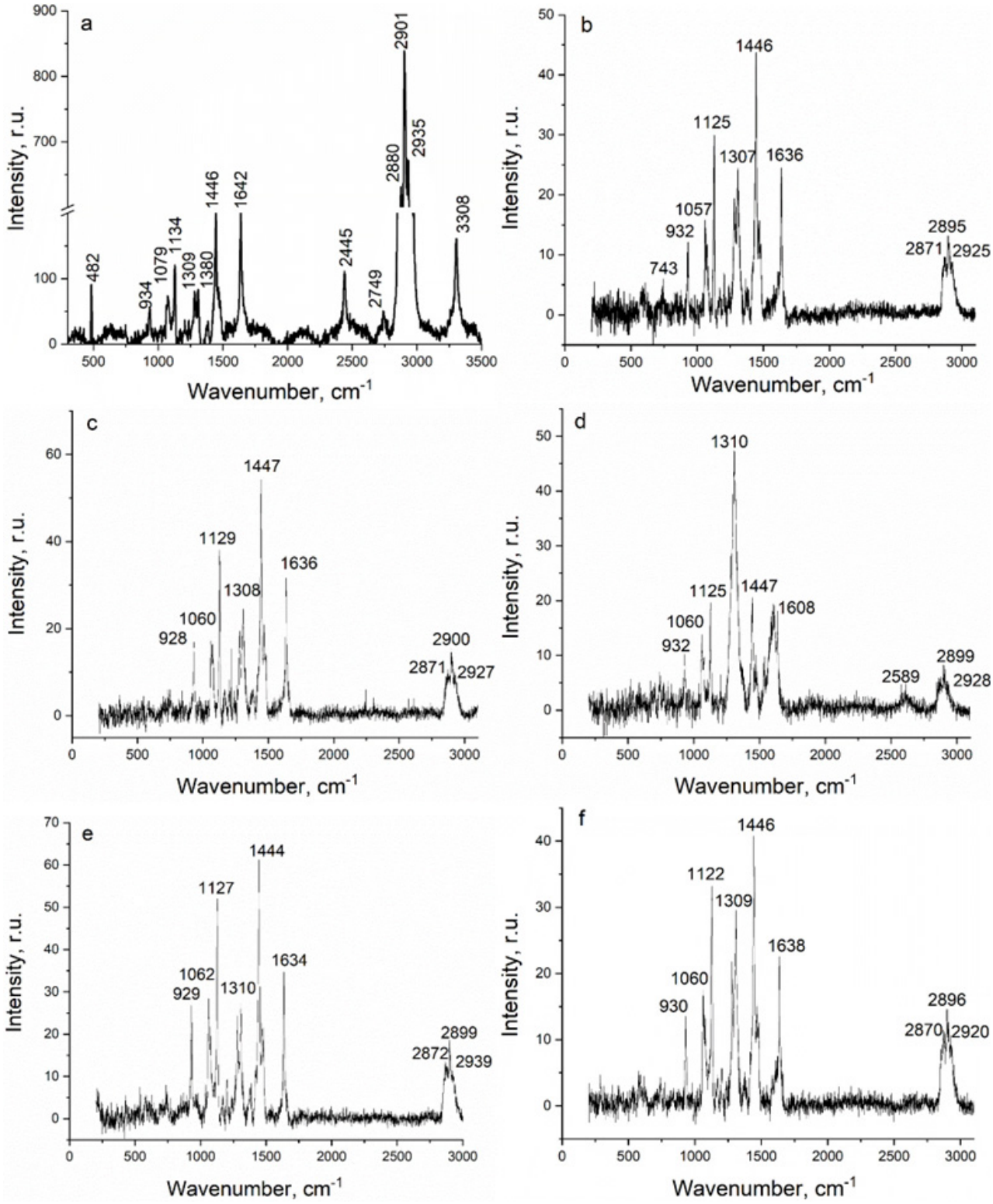

Figure 9. Raman spectra of PA-6/MWCNT nanocomposites with a nanotube content of 0 (a), 0.001 (b), 0.002 (c), 0.005 (d), 0.007 (e), 0.015 vol. pt. (f) after electron irradiation (E_e = 1.8 MeV) with an absorption dose of 10 MRad (100 kGy).

Fig. 10 shows the fast FL spectra for pure PA-6 and PA-6/MWCNT composites after radiation functionalization.

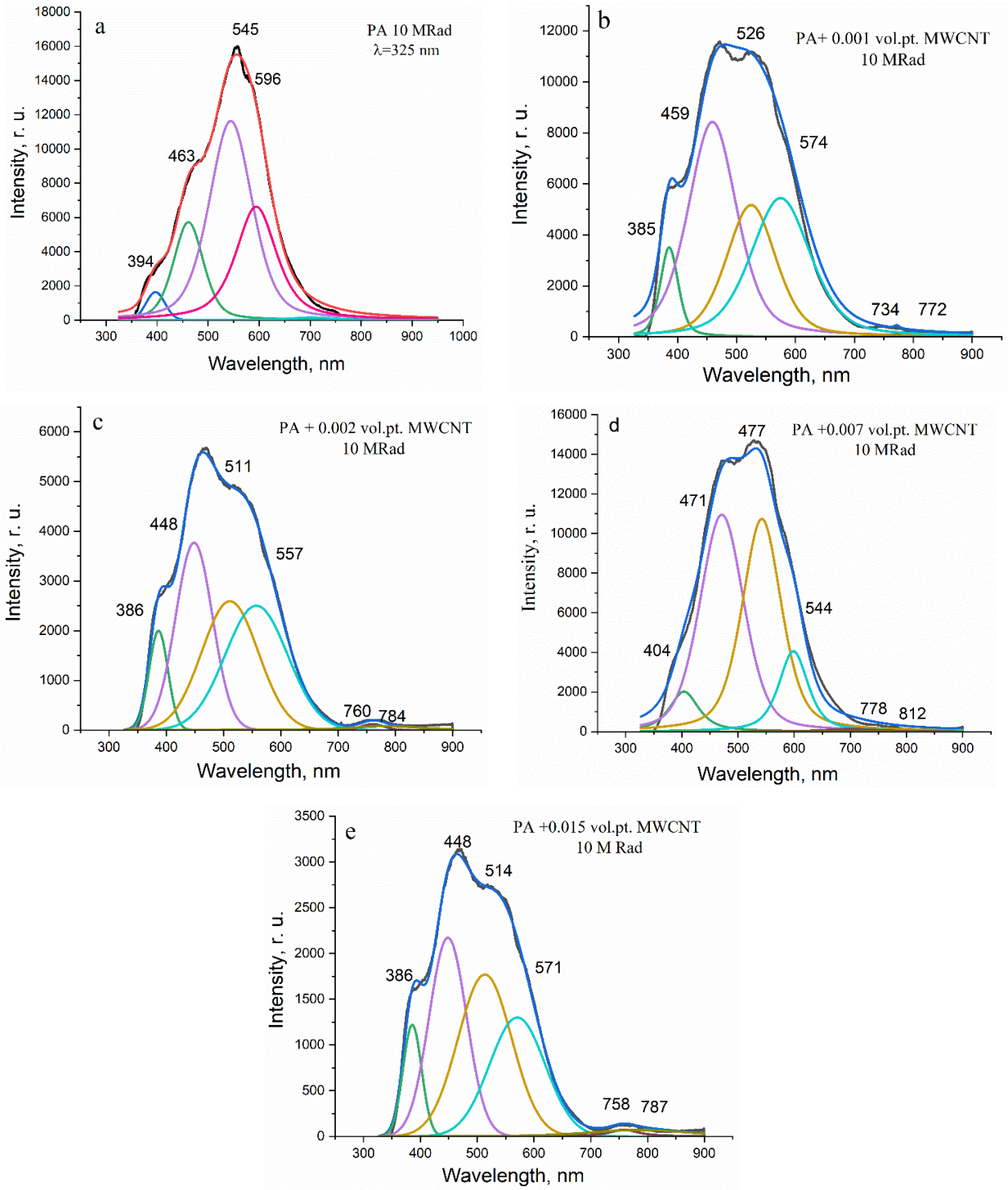

Figure 10. Fast FL spectra of PA-6/MWCNT nanocomposites with a nanotube content of 0 (a), 0.001 (b), 0.002 (c), 0.007 (d), 0.015 vol. pt. (e) after electron irradiation (E_e = 1.8 MeV) with an absorption dose of 10 MRad (100 kGy), individual bands correspond to the fitting components

In the case of pure PA-6, irradiation leads to a restructuring of the FL spectrum, which is manifested in an increase in the intensity of the spectrum. More significant band changes in the FL emission band are observed for the nanocomposite with 0.001 vol. pt. MWCNTs. Thus, for the non-irradiated composite, the main component of the FL band is located at 545 nm (λ_{ex} = 325 nm), and there are also kinks at 391, 467, 606, 742, and 782 nm. Irradiation leads to two main emission components at 459 and 526 nm. The intensity of the components at 385 and 574 nm varies. The introduction of 0.002 vol. pt. MWCNT for the unirradiated polymer composite does not change the shape of the band much. At the same time, irradiation results in the appearance of two components at 448 and 511 nm and kinks at 386 and 557 nm.

For an unirradiated nanocomposite with 0.007 vol. pt. MWCNTs, two main peaks appear at 464 and 540 nm, and two peaks appear at 399 and 598 nm. In the irradiated nanocomposite, two main peaks appear at 471 and 477 nm and two peaks at 404 and 544 nm. Similarly, in the case of the non-irradiated nanocomposite with 0.015 vol. pt. MWCNTs, there are two peaks at 460 and 543 nm and two peaks at 391 and 600 nm. Irradiation at a dose of 10 MRad (100 kGy) is accompanied by a significant band restructuring with the appearance of three components at 386, 448, and 514 nm and a bend at 571 nm.

Thus, the introduction of fillers (MWCNTs) affects the nature of electronic transitions due to the presence of a quasi-continuous spectrum of electron energy, which are local charge states. These local states correspond to the presence of disorder due to the presence of an amorphous phase and defects in the crystal structure. The behavior of the FL spectra shows that in unirradiated composites, the nanotubes have little effect on the rearrangement of the energy levels of the local charge states. It can be assumed that this energy spectrum is primarily determined by the state of the polymer itself. On the other hand, a certain restructuring of the spectra considered with an increase in the CNT content indicates that the nanotubes have a greater effect not on the morphology of the composites, but on the structure of the chains. In this case, the destruction of the chains is possible, accompanied by a decrease in the elastic properties of the Raman scattering spectra. The peculiarity of functionalization of nanocomposites is associated with the effects of electron irradiation with the energy of bombarding charges E_e=1.8 MeV and a dose of 10 MRad (100 kGy). The mechanisms of irradiation have proved to be quite complex and are associated not only with the possible degradation of intramolecular and intermolecular bonds, which in turn determines the energy spectrum of electrons in the interstitial space, as well as the degree of crystallinity of the α-phase.

In addition, electrons can recombine with free radicals formed due to the presence of nanotubes. These mechanisms can also affect the formation of conductive networks and thus lead to a decrease in the percolation threshold.

4. CONCLUSIONS

The preparation of PA-6/MWCNT nanocomposites leads to an increase in the degree of crystallinity with an increase in the content of CNTs, which for this polymer matrix act as nucleation centers of crystallites of a more stable α-phase. With an increase in the concentration of nanotubes in non-irradiated nanocomposites, the effect of electrical conductivity percolation with a percolation threshold of 0.0141 vol. pt. is observed.

Simultaneously, the values of dynamic Young's modulus and shear measured at an ultrasonic frequency of 1 MHz decrease, indicating mechanical damage of polymer macrochains by nanotubes. At the same time, the Raman light scattering spectra are restructured with a shift of most bands and changes in their relative intensity. The fast phase spectra at different MWCNT contents change little, indicating that the nanotubes have little effect on the morphology of the nanocomposites.

As a result, irradiation with electrons of E_e=1.8 MeV with a dose of 10 MRad (100 kGy) and 20 MRad (200 KGy) affects the electrical conductivity (the percolation threshold decreases to 0.0065 vol. pt.), changes the nature of the drop in the dynamic Young's moduli and shear, which is explained by the healing of defects caused by the breakdown of bonds in the circuits by nanotubes.

The destruction of bonds is also indicated by a significant restructuring of the spectra of Raman scattering. For different irradiated PA-6/MWCNT nanocomposites, both the shift of vibrational modes and the restructuring of the relative intensity are observed.

The appearance of intramolecular and intermolecular defects and changes in the amorphous phase occurring during irradiation leads to changes in the energy spectra of local charge states, which in turn affects the behavior of recombination transitions involving local states. As a result of such rearrangement, the fast fluorescence emission spectra for each of the irradiated PA-6/MWCNT nanocomposites change. This, in turn, indicates that these nanocomposites have complex mechanisms of degradation of the intramolecular structure of the presence of fillers, which, on the one hand, form the energy structure within the gap, and, on the other hand, affect changes in the conducting cluster, which leads to a decrease in the percolation threshold in the electrical conductivity of irradiated nanocomposites.

ORCID

Tatiana Pinchuk-Rugal, https://orcid.org/0000-0003-2417-9220; **Oksana Dmytrenko**, https://orcid.org/0000-0002-4271-4234;
Mykola Kulish, https://orcid.org/0000-0002-7409-8560; **Andrii Misiura**, https://orcid.org/0000-0001-9918-1670;
Andriy Momot, https://orcid.org/0000-0001-8162-0161; **Maksim Alieksandrov**, https://orcid.org/0000-0002-9691-5170;
Ihor Danylenko, https://orcid.org/0000-0002-8740-204X; **Yurii Onanko**, https://orcid.org/0000-0002-7231-1188;
Oleksii Melnychenko, https://orcid.org/0000-0002-7787-7674

REFERENCES

[1] T. Arnal, P. Eisenberg, M.J. Abad, A. Ares-Pernas, and C.R. Bernal, "Multifunctional nanocomposites based on a polyamide 6/polyamide 12 blend and multi-walled carbon nanotubes," Polymer Engineering and Science **64**(3), 1246–1257 (2024). https://doi.org/10.1002/pen.26611

[2] J. Arquinto, J. Harada, D.P. De Castro, and L.G. De Andrade E Silva, "Effects of E-Beam irradiation on the chemical, thermal, and mechanical properties of polyamide-6, polyamide-6.6, and polypropylene used in conveyor belt rollers," Materials Research **28**(suppl 1), (2025). https://doi.org/10.1590/1980-5373-MR-2025-0068

[3] P.V. Kodgire, A.R. Bhattacharyya, S. Bose, N. Gupta, A.R. Kulkarni, and A. Misra, "Control of multiwall carbon nanotubes dispersion in polyamide6 matrix: An assessment through electrical conductivity," Chemical Physics Letters **432**(4–6), 480–485 (2006). https://doi.org/10.1016/j.cplett.2006.10.088

[4] B. Krause, P. Pötschke, and L. Häußler, "Influence of small scale melt mixing conditions on electrical resistivity of carbon nanotube-polyamide composites," Composites Science and Technology **69**(10), 1505–1515 (2008). https://doi.org/10.1016/j.compscitech.2008.07.007

[5] H. Li, X. Tuo, B.-H. Guo, J. Yu, and Z.-X. Guo, "Comparison of three interfacial conductive networks formed in carbon Black-Filled PA6/PBT blends," Polymers **13**(17), 2926 (2021). https://doi.org/10.3390/polym13172926

[6] P. Liu, "Modifications of carbon nanotubes with polymers," European Polymer Journal **41**(11), 2693–2703 (2005). https://doi.org/10.1016/j.eurpolymj.2005.05.017

[7] A. Šehić, J. Vasiljević, A. Demšar, M. Leskovšek, V. Bukošek, J. Medved, M. Čolović, I. Jerman, and B. Simončič, "Polyamide 6 composite fibers with incorporated mixtures of melamine cyanurate, carbon nanotubes, and carbon black," Journal of Applied Polymer Science **136**(5), (2018). https://doi.org/10.1002/app.47007

[8] V. Arumugam, A. Góra, and V. Lipik, "Influence of Graphene, Carbon Nanotubes, and Carbon Black Incorporated into Polyamide Yarn on Fabric Properties," Textiles **4**(4), 442–458 (2024). https://doi.org/10.3390/textiles4040026

[9] M. Kaplan, B. Krause, N. Smolka, and I. Kuehnert, "Systematic optimization of conductive PA6/Carbon black nanocomposites through integrated Rheological–Electrical characterization and melt spinning analysis," Fibers and Polymers, (2026). https://doi.org/10.1007/s12221-026-01372-1

[10] A.P. Scott, and L. Radom, "Harmonic Vibrational Frequencies: an evaluation of Hartree−Fock, Møller−Plesset, quadratic configuration interaction, density functional theory, and semiempirical scale factors," The Journal of Physical Chemistry **100**(41), 16502–16513 (1996). https://doi.org/10.1021/jp960976r

[11] S. Huang, T. Liu, W. Zhang, W.C. Tjiu, C. He, and X. Lu, "Grafting polyamide 6 onto multi-walled carbon nanotubes using microwave irradiation," Polymer International **59**(10), 1346–1349 (2010). https://doi.org/10.1002/pi.2873

[12] C. Menchaca, B. Manoun, G. Martínez-Barrera, V.M. Castaño, and H. López-Valdivia, "In situ high-temperature Raman study of crystalline nylon 6,12 fibers gamma-irradiated in argon atmosphere," Journal of Physics and Chemistry of Solids **67**(9–10), 2111–2118 (2006). https://doi.org/10.1016/j.jpcs.2006.05.017

[13] M. Ovsik, M. Stanek, and M. Bednarik, "Evaluation of Cross-Linked Polyamide 6 Micro-Indentation properties: TAIC concentration and electron radiation intensity," Materials **16**(6), 2391 (2023). https://doi.org/10.3390/ma16062391

[14] C. Menchaca, A. Alvarez-Castillo, G. Martinez-Barrera, H. Lopez-Valdivia, H. Carrasco, and V.M. Castano, "Mechanisms for the modification of nylon 6,12 by gamma irradiation," International Journal of Materials and Product Technology **19**(6), 521 (2003). https://doi.org/10.1504/ijmpt.2003.003468

[15] H. Suzuki, S. Ishii, C. Otani, and H. Hoshina, "Low-frequency vibrations of polyamide-6 as a function of temperature and thermal history investigated by terahertz absorption spectroscopy," European Polymer Journal **67**, 284–291 (2015). https://doi.org/10.1016/j.eurpolymj.2015.04.009

[16] M.O. Lisunova, Ye.P. Mamunya, N.I. Lebovka, and A.V. Melezhyk, "Percolation behaviour of ultrahigh molecular weight polyethylene/multi-walled carbon nanotubes composites," European Polymer Journal **43**(3), 949–958 (2006). https://doi.org/10.1016/j.eurpolymj.2006.12.015

[17] Ye.P. Mamunya, V.V. Davydenko, P. Pissis, and E.V. Lebedev, "Electrical and thermal conductivity of polymers filled with metal powders," European Polymer Journal **38**(9), 1887–1897 (2002). https://doi.org/10.1016/s0014-3057(02)00064-2

[18] E. Auyang, M. Ouyang, A. Laycock, H. Blake, T.D. Tetley, T.W. Gant, A.E. Willis, and S. Wright, "Fabrication of microplastic and nanoplastic particles and fibres for use in pulmonary toxicity studies," Particle and Fibre Toxicology **22**(1), 30 (2025). https://doi.org/10.1186/s12989-025-00641-w

[19] M.A. Alieksandrov, T.M. Pinchuk-Rugal, O.P. Dmytrenko, M.P. Kulish, V.V. Shlapatska, and V.M. Tkach, "Radiation-Stimulated Formation of Polyene Structures in Polyethylene Nanocomposites with Multi-walled Carbon Nanotubes," in *Springer Proceedings in Physics*, (2019), pp. 323–332. https://doi.org/10.1007/978-3-030-17759-1_22

[20] T.M. Pinchuk-Rugal, M.P. Kulish, O.P. Dmytrenko, A.I. Momot, A.I. Misiura, M.A. Alieksandrov, V.M. Popruzhko, O.F. Kolomys, and V.V. Shlapatska, "Mechanisms of formation of polyene structures in radiation-functionalized PVC-MWCNT polymer nanocomposites," Vibrational Spectroscopy **125**, 103495 (2023). https://doi.org/10.1016/j.vibspec.2023.103495

[21] M.A. Alieksandrov, A.M. Gaponov, T.M. Pinchuk-Rugal, O.P. Dmytrenko, A. Naumenko, V.M. Popruzhko, and M.P. Kulish, "Conjugate Formation in Films of Polyethylene Glycol and Polypropylene Glycol Nanocomposites with MultiWall Carbon Nanotubes," in *Springer Proceedings in Physics*, (2021), pp. 143–152. https://doi.org/10.1007/978-3-030-74800-5_9

[22] V.M. Popruzhko, O.P. Dmytrenko, M.P. Kulish, T.M. Pinchuk-Rugal, A.I. Misiura, O.L. Pavlenko, A.I. Momot, T.O. Busko, A.P. Onanko, M.A. Alieksandrov, and V.V. Strelchuk, "Electrical and optical properties of polyamide 6 nanocomposites with multi-walled carbon nanotubes," Journal of Molecular Liquids **390**, 123152 (2023). https://doi.org/10.1016/j.molliq.2023.123152

[23] M. Avbar, G.H.M. De Oliveira, and S. De Traglia Amancio-Filho, "Enhancing Mechanical Properties of Polyamide 66 with Carbon-Based Nano-Fillers: A Review," Journal of Composites Science **9**(1), 48 (2025). https://doi.org/10.3390/jcs9010048

[24] M.V. Vasnetsov, "Observation of room-temperature afterglow in Polyamide-6 under UV excitation," Semiconductor Physics Quantum Electronics & Optoelectronics **22**(3), 333–337 (2019). https://doi.org/10.15407/spqeo22.03.333

[25] M.V. Vasnetsov, V.V. Ponevchinsky, D.O. Plutenko, G.V. Klishevich, A.A. Mitryaev, O.I. Gudymenko, and V.P. Kladko, "Luminescence peculiarities of polyamide-6 α and γ forms," Applied Physics B **127**(4), (2021). https://doi.org/10.1007/s00340-021-07601-0

[26] M.D. Murad, B.A. Al-Mayyahi, and A.F.Abbas, "Synthesis and characterization of new fluorescence polyamides," New Materials Compounds and Applications **9**(2), 309-325 (2025). https://doi.org/10.62476/nmca.92309

ЕЛЕКТРИЧНІ, МЕХАНІЧНІ ТА ОПТИЧНІ ВЛАСТИВОСТІ КОМПОЗИТІВ ПОЛІАМІДУ-6 З ВУГЛЕЦЕВИМИ НАНОТРУБКАМИ ПІД ВПЛИВОМ ОПРОМІНЕННЯ

Т.М. Пінчук-Ругаль[1], О.П. Дмитренко[1], М.П. Куліш[1], А.І. Місюра[1,2], А.І. Момот[1], М.А. Алєксандров[3], І.М. Даниленко[3], Ю.А. Онанко[4], О.М. Мельниченко[5]

[1]Київський національний університет імені Тараса Шевченка, вул. Володимирська, 64/13, 01033, Київ, Україна
[2]Інститут електрозварювання ім. Є.О. Патона НАН України, вул. Казимира Малевича, 11, 03150, Київ, Україна
[3]Інститут фізики напівпровідників імені В.Є. Лашкарьова НАН України, проспект Науки, 45, 02000, Київ, Україна
[4]Інститут водних проблем і меліорації НААН, вул. Васильківська, 37, 03022, Київ, Україна
[5]«Радма» Інститут фізичної хімії імені Л. В. Писаржевського НАН України, проспект Науки, 31, 03028, Київ, Україна

Досліджено залежність ступеня кристалічності, динамічного механічного модуля та зсуву на частоті ~1 МГц від вмісту нанотрубок для неопромінених нанокомпозитів ПА-6/БВНТ. Встановлено збільшення ступеня кристалічності та зменшення вказаних модулів зі зростанням вмісту вуглецевих нанотрубок, що пояснюється тим, що вуглецеві нанотрубки в полімерній матриці виступають як центри зарадкоутворення кристалічної α-фази, а також як наночастинки, що руйнують міжатомні зв'язки в ланцюгах та між макромолекулами. Проведено опромінення вказаних нанокомпозитів електронами $E_e \approx 1{,}8$ МеВ з поглинутою дозою 10 МРад (100 кГр) та 20 МРад (200 кГр). Виміряно залежність електропровідності, динамічних механічних модулів, комбінаційного розсіювання та швидкої фотолюмінісценції від вмісту вуглецевих нанотрубок. Показано, що опромінення має складний вплив на вищезазначені властивості. Електрони можуть сприяти як руйнуванню ланцюгів, так і встановленню кристалічної фази, а також загоєнню пошкоджень, спричинених нанотрубками, шляхом рекомбінації електронів з вільними радикалами. Радіаційна функціоналізація широко проявляється в змінах спектрів КРС та енергетичній структурі електронів у забороненій зоні. Ці зміни пов'язані з наявністю локальних станів, зв’язаних з аморфною фазою та структурними дефектами. Це, в свою чергу, проявляється на перебудові спектрів ФЛ і може впливати на формування провідного кластера

Ключові слова: *поліамід-6; нанокомпозити; електропровідність; ступінь кристалічності; динамічні модулі; КРС; флуоресценція; електронне опромінення*